International Journal of Recent Technology and Engineering (IJRTE)
ISSN: 2277-3878 (Online), Volume-9 Issue-1, May 2020

# Multiband Printed Koch Antenna Unified with Hilbert Split-Ring Structure for Better Front-to-Back Ratio

**Ajay Muthuvelan, Ashish Raja Pillai Muthaiah, Twinkle Gopinath Gurusamy, Josephine Pon Gloria Jeyaraj, C. Kalieswari**

***Abstract:*** ***A multiband printed Koch antenna integrated with multi-band high-impedance surface (HIS) is proposed. The antenna can operate at three frequencies like 11.725 GHz, 26.155 GHz and 39.22 GHz which covers application in frequency bands namely X-band (8-12 GHz), K-band (18-27 GHz), and Ka-band (26.5-40 GHz). In order to achieve a modest design with better front-to-back ratio (FBR), gain, directivity and radiation efficiency a multi-band Hilbert split-ring HIS is presented as a reflector. The proposed HIS has an array of slotted square patches based on Hilbert curve. This arrangement provides in-phase reflection at the operating frequencies and can be presented as an artificial magnetic conductor (AMC). The antenna when integrated with HIS has an incorporated uniform profile thickness of 2 mm for different frequencies of operation. The printed Koch antenna is simulated, analyzed for various substrate thickness and is finally integrated with Hilbert split-ring HIS to obtain good FBR and radiation efficiency in all the three bands.***

***Keywords:*** ***Multi-Band Antenna, High-Impedance Surface (HIS), Multi-Band HIS, Modest, Printed Koch Antenna***

## I. INTRODUCTION

In current scenario of development in antenna investigation for applications of wireless communication, multi-band antennas receive more attention [1]–[4]. Many fractal shapes like Hilbert, Sierpinski, Koch, Minkowski and Peano have been used for construction of such multi-band antennas [5]–[12], which established both compactness and multiband behavior. This survey proves the advantages of fractal shapes to design multi-band antennas. Fractal structure naturally has multiple resonances due to coupling between the sharp angles in its geometry and hence it provides different current paths leading to multi-band operation.

Manuscript received on April 02, 2020.
Revised Manuscript received on April 20, 2020.
Manuscript published on May 30, 2020.
* Correspondence Author
**Ajay Muthuvelan***, Department of Electronics and Communication Engineering, National Engineering College (Autonomous), Kovilpatti, Tamil Nadu, India. Email: ajayvijay9398@gmail.com
**Ashish Raja Pillai Muthiah**, Department of Electronics and Communication Engineering, National Engineering College (Autonomous), Kovilpatti, Tamil Nadu, India. Email: ashishkingson007@gmail.com
**Twinkle Gopinath Gurusamy**, Department of Electronics and Communication Engineering, National Engineering College (Autonomous), Kovilpatti, Tamil Nadu, India. Email: twinklegopi01@gmail.com
**Josephine Pon Gloria Jeyaraj***, Department of Electronics and Communication Engineering, National Engineering College (Autonomous), Kovilpatti, Tamil Nadu, India. Email: josephineraj90@gmail.com
**C.Kalieswari**, Department of Electronics and Communication Engineering, National Engineering College (Autonomous), Kovilpatti, Tamil Nadu, India. Email: kalishece@gmail.com



In antennas a planar metallic plate is used as a reflector, which reflects half of the backward radiation in forward direction and thus realizes a better front-to-back ratio. But when this metallic reflector ground is positioned close to the antenna, the image currents get cancelled due to the 180-degree reflection phase of a perfect electric conductor (PEC). So, in order to achieve an interference that is constructive, a quarter wavelength gap between the antenna and metallic reflector ground plane is necessary. However, a multi-band antenna that operates at different frequency bands require different quarter-wavelength gap, which is complicated to be unified by using one perfectly conducting metallic reflector ground plane. This crisis requires a single reflector that can be only several tenths of wavelength from the radiating antenna element. The reflectors with such reflecting characteristics are artificial magnetic conductor (AMC), or electromagnetic band-gap (EBG) structures. In general, the arrangement of periodic metallic unit cells realizes EBG structures. This arrangement makes them to perform exclusive characteristics like in-phase reflection which in turn suppresses surface waves. Due to their distinct characteristics, the HIS and EBG structures have been widely used [13]–[19].

In this paper, a printed Koch antenna is designed to provide multi-band operation. The antenna operates in X-band, K-band, and Ka-band and hence can be used for applications on those bands. In order to achieve better performance in all the three bands with a modest and unified substrate thickness, a multi-band Hilbert split-ring HIS is projected as an AMC reflector, which has etched Hilbert curve slots on an array of square patches. Parametric analysis and studies have been performed to obtain the characteristic properties of the multi-band Hilbert split-ring HIS structure. Also, the multi-band printed Koch antenna with metallic reflectors at different spacing from antenna i.e. 7 mm for X-band, 4 mm for K-band and 2 mm for Ka-band are analyzed. The multi-band printed Koch antenna integrated with Hilbert split-ring HIS with an incorporated profile of 3.85 mm shows better performance when compared to the antenna placed at different gaps from PEC. The prototype of printed Koch antenna with substrate thickness of 2 mm is simulated and measured to validate the design.

## II. DESIGN OF PRINTED KOCH ANTENNA

The design structure of the proposed printed Koch antenna is portrayed as in Fig. 1. The proposed Koch fractal antenna undergoes two iterations and there occurs increment in input resistance of antenna which in turn reduces the resonant frequency. This is due to the increase in length of the fractal segment due to iterations.

The length of the Koch fractal can be obtained [20] using the formula as in (1)

$$PL = PW\left(\frac{4}{3}\right)^n \quad (1)$$

Where, PL is the length, PW is the Koch height and n is the number of iterations.

The proposed antenna uses a microstrip line feed of feed length *FL*= 1.7 mm and feed width *FW*= 0.5 mm. As illustrated in Fig. 1(a), the width ($W_s$) and length ($L_s$) of the ground plane is taken as 8 mm, *PW*=7.5 mm, *n*=2 and *PL*=13.3 mm. of printed Koch antenna with substrate thickness of 2 mm is simulated and measured to validate the design.

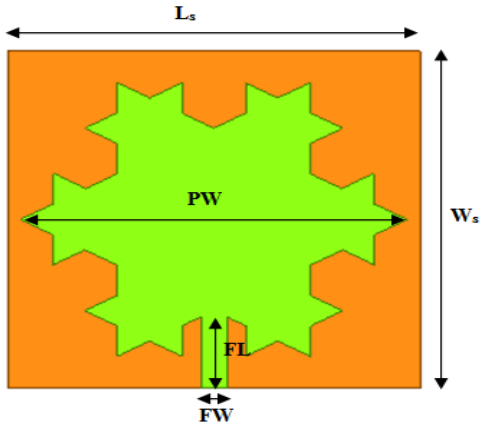


**Fig.1. Design of Printed Koch Antenna**

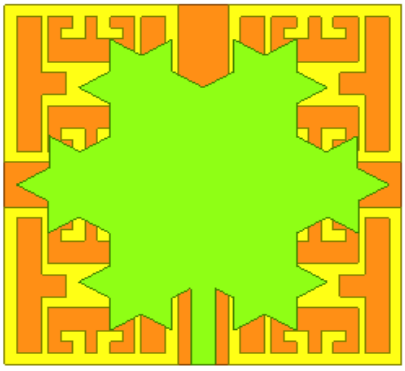

**Fig.2. Design of Printed Koch Antenna integrated with Hilbert Split Ring.**

In order to get a better FBR, a ground plane is placed below the antenna substrate. However, if a metallic planar reflector is used as a ground plane, a minimum thickness of quarter wavelength is required. So, different substrate thicknesses are required for the multi-band printed Koch antenna to operate at different operational frequency bands. The thickness is 2 mm at Ka-band, 4 mm at K-band and 7 mm at X-band. To achieve a unified modest design, this paper presents integration of the printed Koch antenna with multi-band HIS as reflector as shown in Fig. 2. The multi-band HIS has multiple in-phase reflections corresponding to X-, K- and Ka-bands.

## III. DESIGN OF MULTI BAND HILBERT SPLIT RING (HIS) STRUCTURE

The design structure of multi-band Hilbert split-ring HIS is portrayed in Fig. 3, which on top of the substrate consists of 2 X 2 array of Hilbert split-ring slotted square metal patches and on its bottom a planar reflective metal sheet. They are arranged periodically with equal gaps and substrate thickness, and can be perceived as a mushroom-like EBG but without via. Etching a Hilbert based split-ring curve on the square metal patch unit produces multiple in-phase reflection bands. As portrayed in Fig. 3, *W* is the square patch width, *N* is the outer frame width of the square patch, *S* is the space between two splits, *t* is the height of substrate, and $\varepsilon_r$ is the dielectric substrate's permittivity. The Hilbert split-ring HIS design values are calculated and obtained as follows: *W*=3.5 mm, *G*=1 mm, *N*= 0.25 mm, *t*=1.6 mm, *S*= 1 mm and$\varepsilon_r = 3$.

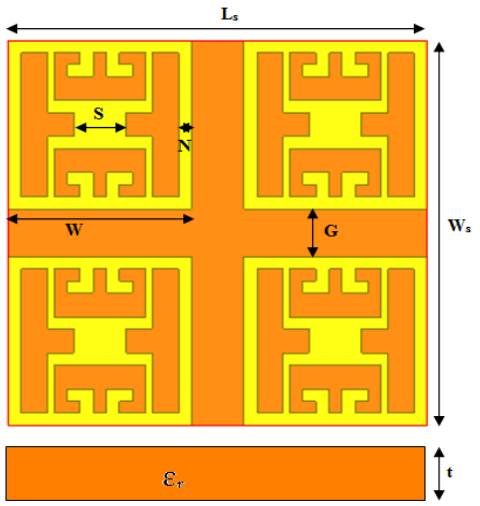


**Fig.3. Geometry of Hilbert Split Ring.**

The EBG/HIS structure can be characterized by means of a parallel LC resonator circuit [17] with a resonant frequency $f = \frac{1}{2\pi\sqrt{LC}}$. The square patch with Hilbert curve based split-ring results in the surface current path length deviation, which provides inductance *L* as depicted in (2). The gap or spacing between two Hilbert split-ring unit cells in the proposed HIS array provides capacitance *C* as given in (3).

$$L = \mu_0\mu_r t \quad (2)$$

$$C = \frac{W\varepsilon_0(\varepsilon_r+1)\cosh^{-1}\left(\frac{W+G}{G}\right)}{\pi} \quad (3)$$

The simulation and analysis were performed using ANSYS HFSS (Ver.17). The Hilbert split-ring EBG surface cancels the image currents and reflects everything at eight frequencies namely 13.6 GHz, 18.3 GHz, 22.5 GHz, 23.9 GHz, 26.4 GHz, 27 GHz, 28 GHz and 37.6 GHz. At these frequencies there occurs abrupt change in reflection phase from positive to negative that adds as special frequencies for the structure. At 15.3 GHz, it transmits the entire incident wave that hits the surface. Fig. 4 shows the reflection, transmission and reflection phase characteristics of the Hilbert split-ring HIS structure.

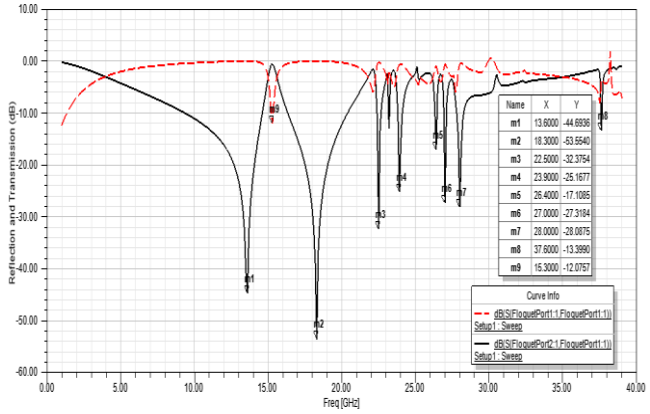


(a)

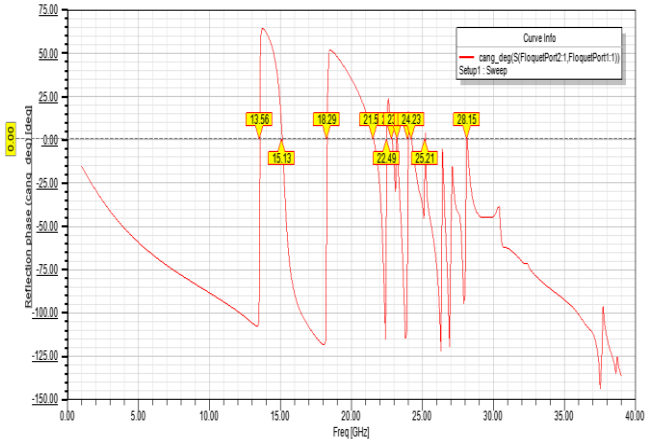


(b)

**Fig.4. (a) Reflection coefficient and Transmission coefficient of Hilbert Split Ring HIS (b) Phase of Reflection - Hilbert Split Ring HIS**

Table 1: Effect of gap width ($G$) on capacitance value

| *G=0.5 mm* | *G=1 mm* | *G=1.5 mm* |
|---|---|---|
| C = 0.8788 pF | C = 0.6006 pF | C = 0.5365 pF |
| f=19.03 GHz | f=21.42 GHz | f=23.14 GHz |

Table 2: Effect of substrate thickness ($t$) on inductance value

| *t =0.8 mm* | *t=1.6 mm* | *t=2.4 mm* |
|---|---|---|
| L = 0.32 nH | L = 0.64 nH | L = 0.96 nH |
| f=30.3 GHz | f=21.42 GHz | f=17.51 GHz |

The gap ($G$) or spacing between the proposed unit cells provides capacitance and its reflection characteristics are analyzed by varying $G$ from 0.5 to 1.5 mm and keeping the height of substrate ($t$) as constant as in Table 1. The frequency shifts to higher frequency band on increasing $G$. This is due to the decrease in the capacitance value ($C$) due to change in gap. The height of substrate ($t$) provides inductance and its reflection characteristics are analyzed by varying $t$ from 0.8 to 2.4 mm and keeping gap ($G$) as constant as in Table 2. The frequency shifts to lower frequency band on increasing $t$. This is due to the increase in the inductance value ($L$) due to change in height of substrate.

## IV. RESULT AND DISCUSSIONS

The radiation characteristics of the printed Koch antenna are analyzed by placing it over a metallic reflector ground plane with different height of substrate like 7 mm for X-band, 4 mm for K-band and 2 mm for Ka-band as shown in Fig.5. But in real scenario the substrate thickness cannot be varied and hence a unified profile thickness is always preferable. So, the printed Koch antenna is integrated with Hilbert split-ring HIS in order to provide unified profile thickness with improved radiation characteristics at all the three bands.

### A. Printed Koch antenna with PEC Ground

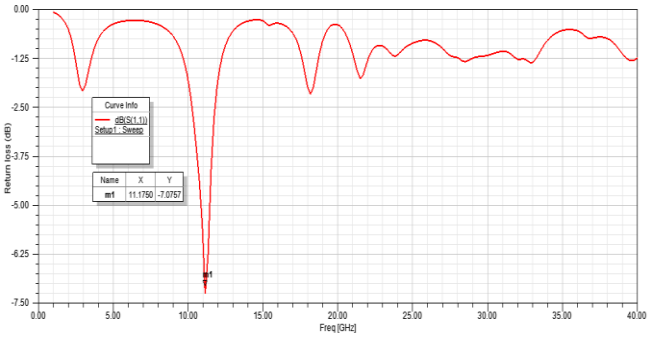


(a)

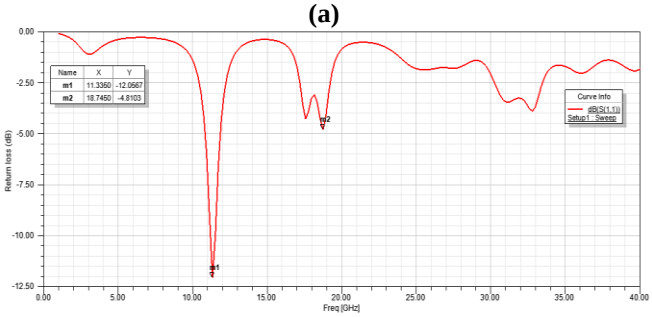


(b)

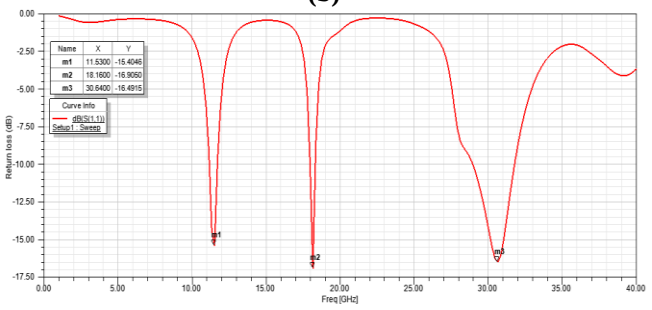


(c)

**Fig.5. Return Loss of Printed Koch Antenna With PEC at different substrate thickness (a) 7 mm, (b) 4 mm, (c) 2 mm.**

The far field radiation parameters are first analyzed by placing the printed Koch antenna over a metallic reflector ground plane with different height of substrate like 7 mm for X-band, 4 mm for K-band and 2 mm for Ka-band.
NIL radiation is usually provided by infinite ground planes in backward direction. But we require finite space antenna element from metallic reflector ground plane in real scenario. Due to this, multipath lobes and nulls are formed at various angles from the edges of ground plane. This reduces the gain and directivity of the proposed antenna due to the wastage of power in the backward direction. Due to poor FBR there occurs backward radiation as shown in Fig. 6.

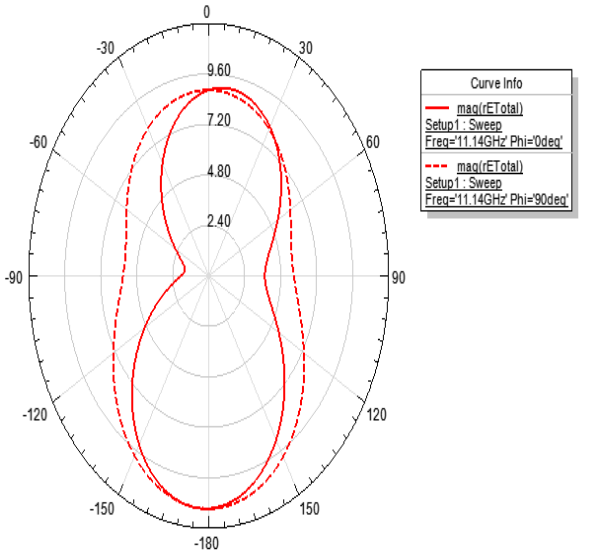


**(a)**

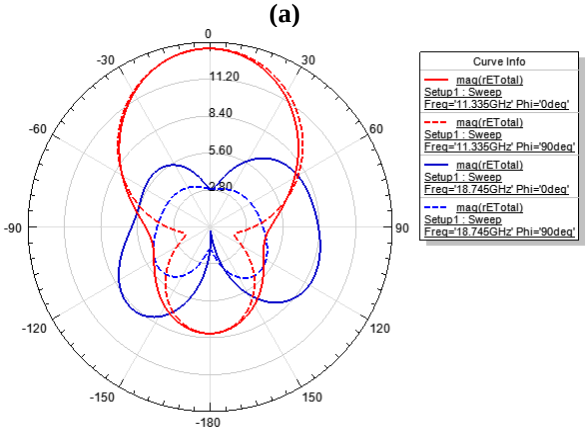


**(b)**

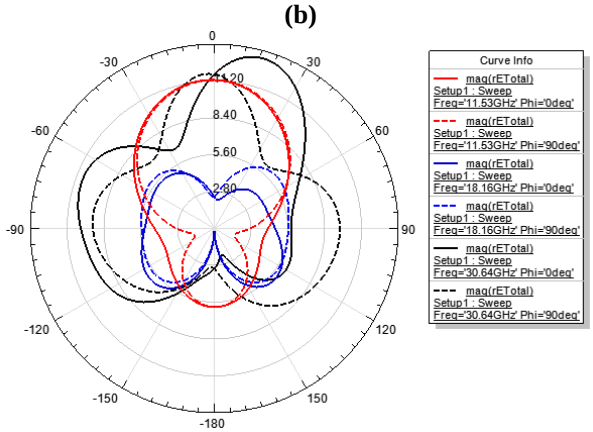


**(c)**

**Fig.6. Radiation Pattern of proposed Printed Koch Antenna with PEC at different substrate thickness (a) 7 mm, (b) 4 mm, (c) 2 mm**

### B. Printed Koch Antenna with Hilbert Split-Ring HIS

Previous analyses show that the multi-band printed Koch antenna needs different heights of substrate for different bands if a metallic planar reflector ground is selected for single direction radiation. Here, a unified substrate thickness of 2 mm for all the three bands by using a Hilbert split-ring HIS structure is used as a ground plane. According to the analysis shown in Fig. 7 and Fig. 8, the printed Koch antenna operates well with 2 mm distance in all the three bands, due to the reflection in in-phase by HIS in X-, K- and Ka-band. Hilbert split-ring HIS structure provides high surface impedances due to inductance and capacitance effect. This in turn suppresses surface wave at the desired frequency band and thereby improves gain, FBR, directivity, and radiation efficiency.

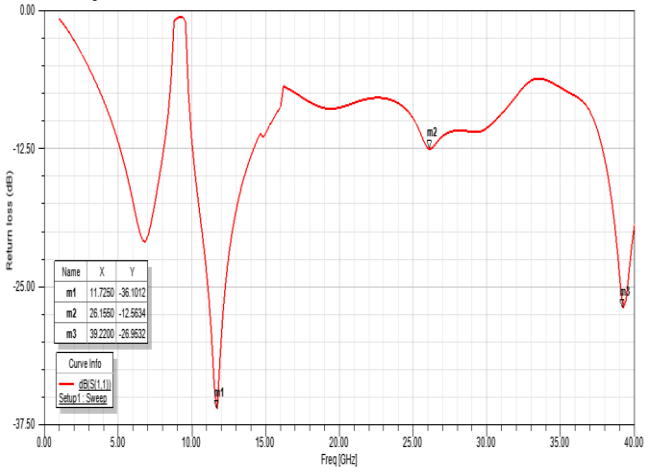


**Fig.7. Return Loss of Printed Koch Antenna with Hilbert Split-Ring HIS**

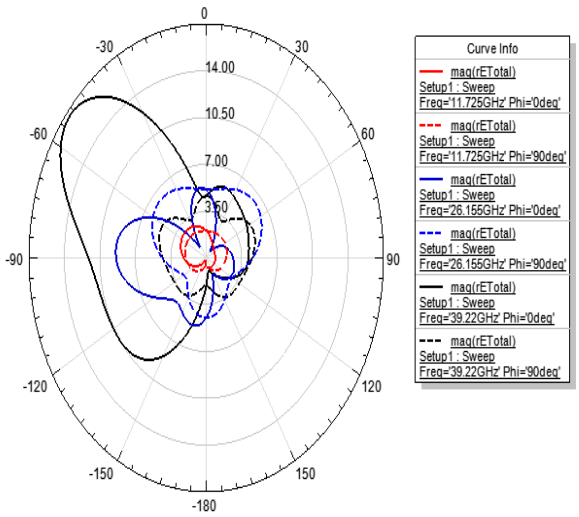


**Fig.8. Radiation Pattern of Printed Koch Antenna with Hilbert Split-Ring HIS**

From Table 3 it is observed that there is improvement in gain by 2 dBi and in directivity by 1.7 dBi for the proposed printed Koch antenna integrated with Hilbert split-ring HIS structure when compared to printed Koch antenna with metallic planar reflector ground plane over a finite distance of 2 mm.

Printed Koch antenna integrated with PEC provides resonance only if they are placed at the corresponding quarter wavelength distance for all the three bands. FBR of the printed Koch antenna improves tremendously by two times when it is backed with HIS. Also, there is a 20% improvement in radiation efficiency of the antenna integrated with HIS. On the whole, the printed Koch antenna integrated with Hilbert split-ring HIS shows improvement in gain and directivity with a good FBR and radiation efficiency.

**Table 3: Comparative Analysis of Radiation Properties of Printed Koch Antenna over PEC and Hilbert Split-Ring HIS**

| *Printed Koch Antenna* | *Resonant frequency (GHz)* | *Return loss (dB)* | *VSWR* | *Gain (dBi)* | *Directivity (dBi)* | *FBR (dB)* | *Radiation efficiency (%)* |
|---|---|---|---|---|---|---|---|
| *With 7 mm thickness* | 11.175 | -7.076 | 2.598 | 6.143 | 7.096 | 1.893 | 80.28 |
| *With 4 mm thickness* | 11.335<br>18.745 | -12.057<br>-4.81 | 1.665<br>3.703 | 7.256<br>5.133 | 8.153<br>6.68 | 4.474<br>3.791 | 87.35<br>70.02 |
| *With 2 mm thickness* | 11.53<br>18.16<br>30.64 | -15.404<br>-16.905<br>-16.491 | 1.409<br>1.333<br>1.352 | 5.535<br>0.416<br>7.049 | 6.952<br>3.28<br>8.137 | 5.537<br>3.278<br>10.465 | 72.15<br>51.70<br>77.84 |
| *With Hilbert split-ring HIS* | 11.725<br>26.155<br>39.22 | -36.101<br>-12.563<br>-26.953 | 1.032<br>1.616<br>1.094 | 7.45<br>3.635<br>9.054 | 8.04<br>4.126<br>9.898 | 10.252<br>10.343<br>17.06 | 96.47<br>89.32<br>82.32 |

## V. CONCLUSION AND FUTURE ENHANCEMENT

A multiband printed Koch antenna integrated with Hilbert split-ring electromagnetic band gap structure is proposed. The antenna can operate at three frequencies like 11.725 GHz, 26.155 GHz and 39.22 GHz which covers application in frequency bands namely X-band (8-12 GHz), K-band (18-27 GHz), and Ka-band (26.5-40 GHz). In order to achieve a modest design with better front-to-back ratio (FBR), gain, directivity and radiation efficiency a multi-band Hilbert split-ring HIS is presented as a reflector. The antenna when integrated with HIS has an incorporated uniform profile thickness of 2 mm for different frequencies of operation. The printed Koch antenna is simulated, analyzed for various substrate thickness and is finally integrated with Hilbert split-ring HIS to obtain good FBR and radiation efficiency in all the three bands. Introducing switches in HIS for frequency reconfiguration can further extend this work.

## REFERENCES


1. Xu Y, Jiao YC, Luan YC (2012), "Compact CPW-fed printed monopole antenna with triple-band characteristics for WLAN/WiMAX applications", Electronics Letters, 48(24):1519–1520.
2. Abutarboush HF, Nasif H, Nilavalan R, Cheung SW (2012), "Multiband and Wideband Monopole Antenna for GSM900 and Other Wireless Applications", IEEE Antennas and Wireless Propagation Letters, 11:539–542.
3. Basaran SC (2010), "Dual wideband CPW-fed split-ring monopole antenna for WLAN applications", In: 2010 10th Mediterranean Microwave Symposium, IEEE, p. 174–177.
4. Park SI, Lee J (2012), "A multiband film type inverted F-antenna for GSM, DCS, PCS, USPCS, and WCDMA bands", Microwave and Optical Technology Letters, 54(12):2757–2762.
5. Yogesh Kumar Choukiker, Satish K. Sharma, and Santanu K. Behera (2014), " Hybrid Fractal Shape Planar Monopole Antenna Covering Multiband Wireless Communications With MIMO Implementation for Handheld Mobile Devices" IEEE Transactions On Antennas And Propagation, Vol. 62, No. 3.
6. S. Oraizi and H. Hedayati (2011), "Miniaturized UWB monopole microstrip antenna design by the combination of Giuseppe Peano and Sierpinski carpet fractals," IEEE Antennas Wireless Propagation Letters, vol. 10, pp. 67–70.
7. Y. K. Choukiker and S. K. Behera (2011), "Design of wideband fractal antenna with combination of fractal geometries," in Proc. IEEE 8th Int. Conf. on Information, Communications, and Signal Processing (ICICS 2011), Singapore, pp. 1–4, Dec. 13–16.
8. W.-L. Chen, G.-M. Wang, and C.-X. Zhang (2008), "Small-size microstrip patch antennas combining Koch and Sierpinski fractal-shapes," IEEE Antennas Wireless Propagation Letters, vol. 7, pp. 738–741.
9. L. Lizzi and G. Oliveri (2010), "Hybrid design of a fractal-shaped GSM/UMTS antenna," J. Electromagnetic. Waves Applications, vol. 24, no. 5, pp. 707–719.
10. J. Anguera, C. Puente, C. Borja, and R. Montero (2001), "Bowtie microstrip patch antenna based on the Sierpinski fractal," in Proc. IEEE Int. Symp. Antennas and Propagation Society, vol. 3, pp. 162–165.
11. C. Puente-Baliarda, J. Romeu, R. Pous, and A. Cardama (1998), "On the behavior of the Sierpinski multiband fractal antenna," IEEE Trans. Antennas Propagation, vol. 46, no. 4, pp. 517–524.
12. J.Anguera,C.Puente,C.Borja,R.Montero,andJ.Solder (2001),"Small and high-directivity bow-tie patch antenna based on the Sierpinski fractal," Microwave Opt. Technol. Letters, vol. 31, no. 3, pp. 239–241.
13. X. Chen, L. Li, C.-H. Liang, and Z.-J. Su (2010), "Locally resonant cavity cell model for meandering slotted electromagnetic band gap structure," IEEE Antennas Wireless Propagation Letters, vol. 9, pp. 3–7.
14. X. Chen, L. Li, C.-H. Liang, Z.-J. Su, and C. Zhu (2012), "Dual-band high impedance surface with mushroom-type cells loaded by symmetric meandered slots," IEEE Trans. Antennas Propagation, vol. 60, no. 10, pp. 4677–4687.
15. S. Z. Zhu and R. Langley (2009), "Dual-band wearable textile antenna on an EBG substrate," IEEE Trans. Antennas Propagation, vol. 57, no. 4, pp. 926–935.
16. L.Li, Q.Chen, Q.W.Yuan, C.H.Liang, and K.Sawaya (2008),"Surface wave suppression band gap and plane-wave reflection phase band of mush- room-like photonic band gap structures," Journal of Applied Physics, vol. 103, no. 023513.
17. D. F. Sievenpiper, L. Zhang, R. F. J. Broas, N. G. Alexopolus, and E. Yablonovitch (1999), "High-impedance electromagnetic surfaces with a for- bidden frequency band," IEEE Trans. Microwave Theory Tech., vol.47, no. 11, pp. 2059–2074.
18. F. Yang and Y. Tahmat-Sammi (2003), "Reflection phase characterizations of the EBG ground plane for low profile wire antenna application," IEEE Trans. Antennas Propagation, vol. 51, no. 10, pp. 2691–2703.
19. D. Qu, L. Shafai, and A. Foroozesh (2006), "Improving microstrip patch antenna performance using EBG substrates," in IEE Proc. Microwave. Antennas Propagation, vol. 153, pp. 558–563.
20. Simarpreet Kaur, Rajni, and Anupma Marwaha (2014), "Fractal Antennas: A Novel Miniaturization Technique for Next Generation Networks", International Journal of Engineering Trends and Technology, Vol. 9, pp. 744-747.


## AUTHORS PROFILE

**Ajay Muthuvelan** is an Under Graduate student in Department of ECE at National Engineering College (Autonomous), Tamil Nadu, India. His research area includes RF and Microwave Communication.

**Ashish Raja Pillai Muthiah** is an Under Graduate student in Department of ECE at National Engineering College (Autonomous), College, Tamil Nadu, India. His research area includes RF and Microwave Communication.

**Twinkle Gopinath Gurusamy** is an Under Graduate student in Department of ECE at National Engineering College (Autonomous), Tamil Nadu, India. His research area includes RF and Microwave Communication.

**Dr. Josephine Pon Gloria Jeyaraj** received her B.E. Degree in Electronics and Communication Engineering, M.E. Degree in Communication Systems and Ph.D. in Antenna Design. Her research area includes RF and Microwave Communication, Wireless Communication.

**Mrs. C. Kalieswari** received her B.E. Degree in Electronics and Communication Engineering and M.E. Degree in VLSI Design. Her research area includes VLSI Design, RF and Microwave Communication.

*Retrieval Number: F9189038620/2020©BEIESP*
*DOI:10.35940/ijrte.F9189.059120*
*Journal Website: www.ijrte.org*



*Published By:*
*Blue Eyes Intelligence Engineering*
*& Sciences Publication*